Effect of Soluble Tissue Factor on the Kinetic Mechanism of Factor VIIa: Enhancement of *p*-Guanidinobenzoate Substrate Hydrolysis†

Marvin A. Payne,‡,§ Pierre F. Neuenschwander,§ Arthur E. Johnson,|| and James H. Morrissey*,§

Department of Chemistry and Biochemistry, University of Oklahoma, Norman, Oklahoma 73019, Cardiovascular Biology Research Program, Oklahoma Medical Research Foundation, Oklahoma City, Oklahoma 73104, and Department of Medical Biochemistry & Genetics, Texas A&M University Health Science Center, College Station, Texas 77843

Received December 18, 1995; Revised Manuscript Received March 20, 1996⊗

ABSTRACT: The mechanism by which the protein cofactor, tissue factor, enhances the activity of its cognate serine protease, coagulation factor VIIa (FVIIa), has been studied using the fluorogenic ester substrate 4-methylumbelliferyl *p*′-guanidinobenzoate (MUGB). Kinetic data were collected at pH 8.4 and pH 7.6 in the presence and absence of soluble tissue factor (sTF; recombinant human tissue factor containing only the extracellular domain). Pre-steady-state techniques allowed the determination of the individual rate constants for acylation (k_2) and deacylation (k_3) of the sTF·FVIIa complex as well as the dissociation constant for the noncovalent Michaelis complex with MUGB. Alternative methods were required for determination of these parameters for free FVIIa due to extremely slow hydrolysis of MUGB in the absence of sTF. Under all experimental conditions, deacylation was found to be rate-limiting. The major effect of sTF was to raise the affinity of FVIIa for MUGB (31-fold at pH 8.4 and 36-fold at pH 7.6); only minor changes in k_2 and k_3 were observed. Thus, we conclude that for the ester substrate MUGB, sTF exerts greater allosteric effects on substrate binding than on the later steps involved in the catalytic pathway.

Factor VIIa (FVIIa),[1] a trypsin-like serine protease, is the initiating enzyme in the blood coagulation cascade and is responsible for triggering blood clotting in both normal hemostasis and thrombotic disease [reviewed by Carson and Brozna (1993)]. FVIIa has very little enzymatic activity in the absence of TF, its obligatory protein cofactor. TF is a relatively small integral membrane protein with a single membrane-spanning domain. The X-ray crystal structure of the isolated extracellular domain (the portion which binds FVIIa) has recently been solved, confirming that TF is a member of the cytokine/growth factor receptor family (Harlos et al., 1994; Muller et al., 1994).

Binding of FVIIa to TF causes an enormous increase in the catalytic activity of FVIIa toward its natural macromolecular substrates (FVII, FIX, and FX). Full enhancement of FVIIa proteolytic activity requires that TF be incorporated into phospholipid vesicles (Bom & Bertina, 1990; Bom et al., 1990) which are composed, ideally, of a mixture of neutral and acidic phospholipids. The magnitude of the rate enhancement for FVIIa binding to phospholipid-embedded TF is over 10^6-fold (Bom & Bertina, 1990). Binding of FVIIa to TF also causes a substantial increase in the rate of hydrolysis of small, tripeptidyl-amide and -ester substrates (Zur & Nemerson, 1978; Higashi et al., 1992; Lawson et al., 1992; Butenas et al., 1993). The magnitude of this latter effect is about 40−120-fold, and does not require TF to be embedded in phospholipid vesicles (Krishnaswamy, 1992). Thus, protein−protein interactions between TF and FVIIa are themselves sufficient for TF to act as an allosteric regulator of the active center of FVIIa, enabling this aspect of TF cofactor function to be studied using either TF in phospholipid vesicles or TF solubilized in detergent.

Recently, a soluble mutant form of TF (sTF; the extracellular domain of TF) has been produced by recombinant means (Ruf et al., 1991a; Rezaie et al., 1992; Shigematsu et al., 1992; Waxman et al., 1992). This form of TF is especially advantageous for studying the allosteric regulation of FVIIa by TF because sTF is highly water-soluble (Waxman et al., 1992), retains full cofactor activity toward FVIIa amidolytic activity (Ruf et al., 1991b), and can be produced in high yield in bacteria (Rezaie et al., 1992). While it was originally thought that sTF was defective in supporting the activation of FX by FVIIa (Waxman et al., 1992), it was subsequently shown that this apparent defect of sTF was directly attributable to the weak affinity of the sTF·FVIIa complex for phospholipid surfaces (Fiore et al., 1994). Since activation of FX (or FIX) is a highly surface-dependent reaction, when conditions are used which promote quantitative binding of sTF·FVIIa to phospholipids, this soluble form of the enzyme−cofactor complex supports rates of macromolecular substrate activation equivalent to those of the wild-type TF·FVIIa complex (Fiore et al., 1994). This finding

† This study was supported in part by National Institutes of Health Grants F32 HL09091 (M.A.P.) and R01 HL47014 (J.H.M.), by the Robert A. Welch Foundation (A.E.J.), and by a Grant-in-Aid from the American Heart Association (P.F.N.).

* To whom correspondence should be addressed at the Cardiovascular Biology Research Program, Oklahoma Medical Research Foundation, 825 NE 13th St., Oklahoma City, OK 73104. Telephone: (405) 271-7892. Facsimile: (405) 271-3137. E-mail: morrisseyj@omrf.uokhsc.edu.

‡ University of Oklahoma.

§ Oklahoma Medical Research Foundation.

|| Texas A&M University Health Science Center.

⊗ Abstract published in *Advance ACS Abstracts,* May 15, 1996.

[1] Abbreviations: BSA, bovine serum albumin; TF, tissue factor; sTF, recombinant soluble tissue factor; FVII, zymogen form of clotting factor VII; FVIIa, active form of clotting factor VII; GB-FVIIa, covalent *p*-guanidinobenzoyl-factor VIIa acyl-enzyme complex; FXa, active form of clotting factor X; MUGB, 4-methylumbelliferyl *p*′-guanidinobenzoate; *p*NPGB, *p*-nitrophenyl *p*′-guanidinobenzoate; Chromozym t-PA, $MeSO_2$-D-phenylalanylglycylarginyl-*p*-nitroanilide acetate; pps, pulses per second.

S0006-2960(95)02977-1 CCC: $12.00

adds confidence that studies using sTF to promote allosteric activation of FVIIa faithfully reflect the protein−protein component of the interactions between wild-type TF and FVIIa. Furthermore, it allows protein−protein interactions between FVIIa and TF to be studied without the potentially complicating effects of phospholipid or detergent.

Numerous studies have focused on the mechanism of action of TF in enhancing the catalytic activity of FVIIa [reviewed in Rapaport (1991) and Carson and Brozna (1993)]. With respect to activity toward synthetic amide and ester substrates, kinetic data have been collected by several groups showing that TF causes an increase in k_{cat} ranging in magnitude from roughly 6- to 150-fold (Shigematsu et al., 1992; Higashi et al., 1992; Neuenschwander et al., 1993; Butenas et al., 1993). For some peptidyl-amide substrates, TF also causes up to a 5-fold decrease in K_m (Neuenschwander et al., 1993). Thus, depending on the substrate, TF increases the k_{cat}/K_m ratio roughly 40−150-fold. In spite of these studies, the mechanism of allosteric activation of FVIIa by TF remains unclear. This is also true for the other blood coagulation enzymes whose cognate protein cofactors are all known to be essential for expression of full clotting activity. With respect to FVIIa and TF, the effects of TF on the kinetics of hydrolysis of synthetic substrates by FVIIa have yet to be fully described in the context of the probable chemical mechanism for FVIIa.

Esters of *p*-guanidinobenzoate were originally developed as active site titrants for trypsin-like proteases (Chase & Shaw, 1967; Bock et al., 1989), and have proven useful as mechanistic probes of various serine proteases (Jameson et al., 1973; Smith, 1973; Livingston et al., 1981; Melhado et al., 1982). In most cases, this is primarily due to the relatively slow rates of acylation and deacylation of ester substrates, allowing convenient estimation of the individual rate constants along the reaction pathway. In this paper, we address the effects of sTF on the kinetic mechanism of FVIIa for the fluorogenic ester substrate MUGB (Jameson et al., 1973). The formation of the *p*-guanidinobenzoyl-FVIIa (GB-FVIIa) acyl-enzyme intermediate occurs on a time scale of several minutes, with very slow hydrolysis of the intermediate. Thus, MUGB hydrolysis by FVIIa can be conveniently observed in both the pre-steady-state and steady-state, allowing the processes of substrate binding, enzyme acylation, and enzyme deacylation to be studied independently. We present data on the hydrolysis of this substrate for both free FVIIa and the sTF·FVIIa complex, and discuss the effect of sTF on the individual rate constants along the FVIIa catalytic pathway.

EXPERIMENTAL PROCEDURES

Reagents. MUGB was obtained from Sigma Chemical Co. (St. Louis, MO), and Chromozym t-PA was from Boehringer Mannheim (Indianapolis, IN). All other reagents were of the highest quality available from various suppliers.

Protein Purification. Human FVII was purified from plasma and activated to FVIIa using FXa−agarose as previously described (Neuenschwander & Morrissey, 1992). The FVIIa was dialyzed exhaustively into 50 mM Hepes−NaOH, pH 7.5, containing 100 mM NaCl before use in fluorescence assays. Human sTF was expressed in *Escherichia coli* and purified as previously described (Rezaie et al., 1992).

Fluorimetric Assays. Assays of FVIIa enzymatic activity using the fluorogenic substrate MUGB were carried out using an SLM 8000C fluorimeter (SLM Instruments; Rochester, NY) equipped with a 450-W xenon light source and a cooled photomultiplier tube housing. The excitation and emission wavelengths were set at 365 nm and 445 nm, respectively, with a band-pass of 4 nm. Sample emission intensities were measured in the photon-counting mode and are expressed as pulses per second (pps). The background intensity of each sample before addition of MUGB has been subtracted in all cases.

Assays were done in 3-mL quartz cuvettes in buffer containing 100 mM NaCl and 5 mM $CaCl_2$ with either 50 mM barbital, pH 8.4 (buffer B), or 50 mM Hepes−NaOH, pH 7.6 (buffer H). Typically, sTF (490 nM final concentration) was added to 2 mL of buffer in a cuvette with continuous stirring. MUGB (dissolved in DMSO; <1% final) was then added, and the blank rate of MUGB hydrolysis (in the absence of FVIIa) was followed for approximately 150 s before addition of FVIIa to a final concentration of 97 nM. In each instance, the dead time for addition of the FVIIa was about 10 s. The fluorescence intensity was then monitored for an additional 1500−1800 s, and the contribution of the blank to the fluorescence intensity was subtracted from each time point by extrapolation of the initial measured blank rate. The amount of MUGB spontaneously hydrolyzed during an assay was found to be less than 1%, while the maximum amount of MUGB hydrolyzed enzymatically was roughly 10%. Under all assay conditions, the absorbance of MUGB was too low to cause measurable inner filter effects.

Chromogenic Assays. Inhibition assays of the chromogenic activity of FVIIa and the sTF·FVIIa complex in the presence of various concentrations of MUGB were performed using Chromozym t-PA substrate (Neuenschwander et al., 1993) and buffer B containing either 0.1% (w/v) PEG-8000 or 0.1% (w/v) BSA. The concentration of FVIIa was either 200 nM in the absence of sTF or 10 nM in the presence of 500 nM sTF. The MUGB and Chromozym t-PA were premixed before the addition of FVIIa ± sTF to yield the indicated final concentrations. Reaction volumes were 100 μL, and initial rates of substrate hydrolysis were determined at ambient temperature using a Vmax kinetic microplate reader (Molecular Devices; Menlo Park, CA) in untreated polystyrene 96-well microplates (Corning, NY).

For independent determination of the rate of deacylation of acyl-enzyme intermediates, the following two-stage assay was used. In the first stage, the acyl-enzyme was prepared in buffer B or H by mixing FVIIa (1.8 μM final) with MUGB (100 μM final) either in the absence or in the presence of sTF (10 μM final) and allowing the mixture to incubate for 1 h at ambient temperature. The second stage of the reaction consisted of a 100-fold dilution of the acyl-enzyme mixture in the appropriate buffer containing 0.1% (w/v) BSA followed by measurement of the recovery of enzyme activity in a chromogenic assay using 5 mM Chromozym t-PA. For assays in the presence of sTF, the final assay mixture was supplemented with sTF to yield a final concentration of 400 nM. Control reactions performed under identical conditions in the absence of MUGB showed no change in enzyme activity over the time course of an assay.

Data Analysis, General. Unless indicated otherwise, numerical analyses of kinetic data were performed by

nonlinear least-squares methods using Powell's algorithm with Gauss−Newton and Steepest Descent corrections, as implemented by SCIENTIST (MicroMath Scientific Software; Salt Lake City, UT) for fitting directly to differential equations. Fitted values are reported ± the standard error of the fitted function to the data. Data sets obtained at more than one reactant concentration were fit globally using the entire data set. The general kinetic methods used in this study have been used successfully in studies of other serine proteases (Kezdy & Bender, 1962; Bender et al., 1967; Jameson et al., 1973; Wohl et al., 1978; Bock et al., 1989). An explanation of how these theories and kinetic methods were applied to FVIIa and the sTF·FVIIa complex, and the equations used for fitting, is described below.

Analysis of Fluorescent Substrate Assays. The working kinetic model used to analyze time-dependent fluorescence and activity data using MUGB as the substrate is given by Scheme 1.

Scheme 1

$$E + S \overset{K_s}{\rightleftharpoons} E{\cdot}S \xrightarrow{k_2} ES' + P_1 \xrightarrow{k_3} E + P_2$$

In this model, S represents substrate, E represents enzyme, P_1 represents the first product released (assumed to be the fluorophore or chromophore, in this case 4-methylumbelliferone or *p*-nitrophenol), P_2 represents the second product released (*p*-guanidinobenzoate), ES′ represents the acyl-enzyme (guanidinobenzoyl-enzyme) intermediate, K_s is the dissociation constant for the noncovalent E·S complex, k_2 is the first-order rate constant for acylation, and k_3 is the first-order rate constant for deacylation.

Assuming $[S]_0 \gg [E]_0$ and that S binds in rapid equilibrium, the following differential equation can be derived to describe the formation of P_1 as a function of time (Bender et al., 1967):

$$\frac{d[P_1]}{dt} = \frac{k_2[E]_0 - k_2(a/b)(1 - e^{-bt})}{1 + K_s/[S]_0} \quad (1)$$

where $[E]_0$ is the initial concentration of enzyme, $[S]_0$ is the initial concentration of substrate, and *a* and *b* are defined as follows:

$$a = \frac{k_2[E]_0}{1 + K_s/[S]_0} \quad (2)$$

$$b = k_3 + \frac{k_2}{1 + K_s/[S]_0} \quad (3)$$

One can integrate eq 1 to obtain:

$$[P_1] = \frac{k_2[E]_0 - k_2(a/b)}{1 + K_s/[S]_0}t + \frac{k_2 a}{b^2(1 + K_s/[S]_0)}(1 - e^{-bt}) \quad (4)$$

which is of the general form

$$[P_1] = At + B(1 - e^{-bt}) \quad (5)$$

where parameters *A* and *B* are bulk constants from eq 4, and *b* is as defined in eq 3.

Individual fluorescence time courses were fit with eq 5 to obtain the bulk constants *A* and *B*. Graphical methods were then used to obtain initial estimates of the kinetic parameters k_2, k_3, and K_s as described by Bender et al. (1967). These initial estimates were then used for the final global fitting procedure of the entire data set using eq 1 to obtain refined kinetic parameters for the model.

Analysis of Deacylation Data. The kinetic model for measurement of deacylation of an acyl-enzyme by regaining the active enzyme can be written as Scheme 2

Scheme 2

$$E^* \xrightarrow{k_3} E + S_2 \overset{K_{s_2}}{\rightleftharpoons} ES_2 \xrightarrow{k_5} E + P$$

where E* is the inactive acyl-enzyme, E is active free enzyme, ES_2 is the binary complex between E and S_2 (the rapidly-hydrolyzed second substrate, Chromozym t-PA in this case), P represents the combined products of the hydrolysis of S_2, k_3 is the first-order rate constant for deacylation, K_{s_2} is the dissociation constant for the ES_2 complex, and k_5 is the pseudo-first-order rate constant reflecting all the catalytic steps associated with S_2 hydrolysis and product release. The rate of this reaction can be described by a series of differential equations which integrate to the form of eq 6 where parameters *C* and *D* are defined by eqs 7 and 8 (Wohl et al., 1978).

$$[P] = [P]_0 + Ct + (C - D)(e^{-k_3 t} - 1) \quad (6)$$

$$C = \frac{k_5[S_2][E]_{tot}}{K_s} \quad (7)$$

$$D = \frac{k_5[S][E]_0}{K_s} \quad (8)$$

Equation 6 was fit directly to time-course data for the recovery of enzymatic activity in a chromogenic assay (*cf.* Figure 5).

RESULTS

Kinetic Parameters of MUGB Hydrolysis by the sTF·FVIIa Complex. The fluorescence-detected hydrolysis of MUGB by sTF·FVIIa for a typical experiment is shown in Figure 1 at a single MUGB concentration along with a plot of the best-fit curve using eq 5. Parameter *B* in eq 5 is mathematically equivalent to $[E]_0$ under conditions of infinite $[S]_0$, and where $k_3 \approx 0$. Under the above conditions, the enzyme goes through a single catalytic turnover and becomes effectively locked in the acyl-enzyme intermediate. Thus, if the net fluorescence intensity developed in the assay is calibrated to an external concentration standard, the determined value of parameter *B* will allow active-site titration of the enzyme. In the case of sTF·FVIIa, the *y*-intercept of a regression-line of the linear portion of a time course yields a value for parameter *B* which approximates the fluorescence intensity developed by stoichiometric reaction of MUGB with enzyme (sTF·FVIIa). In this case, extrapolation of the linear portion of the assay to the ordinate yields a value for parameter *B* which is a complex function of $[E]_0$ but which can nonetheless be used to extract $[E]_0$ using appropriate transformations of the data (Bender et al., 1967; Chase & Shaw, 1969). Since

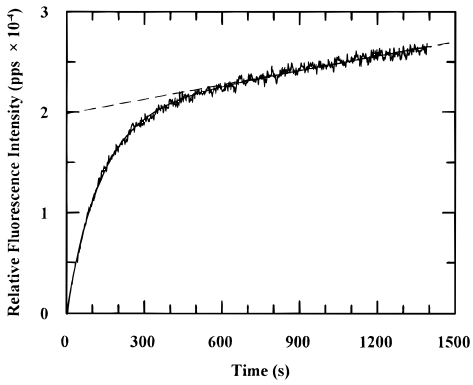

FIGURE 1: Typical time course for the hydrolysis of MUGB by sTF·FVIIa. The net fluorescence intensities shown here were obtained by subtracting both the initial background fluorescence and the time-dependent fluorescence due to the spontaneous hydrolysis of MUGB from the observed intensities. The conditions of the assay were as described under Experimental Procedures at pH 7.6 using 7.2 μM MUGB. The curve was obtained by fitting eq 5 to the entire time course. The parameters *A*, *B*, and *b* were extracted from the fit of eq 5 to the data and used for subsequent analysis. The dashed line was obtained by linear regression of the time course from 600 s to 1390 s and is shown for illustrative purposes only (see text).

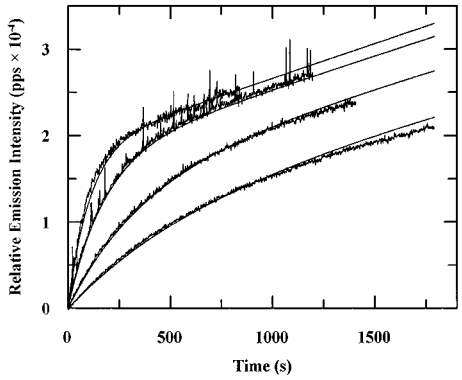

FIGURE 2: Effect of varying [MUGB] on the hydrolysis of MUGB by sTF·FVIIa. The fluorescence data were obtained as for Figure 1 at pH 8.4. The concentrations of MUGB used were (from bottom to top) 0.72 μM, 1.4 μM, 3.6 μM, and 7.2 μM. The curves are from a fit of eq 1 to the entire data set as described under Experimental Procedures. $[E]_0$ was 97 nM. When fully acylated, this concentration of enzyme yielded a fluorescence intensity of 2.03×10^4 pps based on the fit of eq 1. Reciprocal weighting was used for fitting to better define the pre-steady-state parameters. Values for the kinetic parameters are given in Table 1. The intermittent spikes observed in the fluorescence trace for 3.6 μM MUGB are due to dust particles in the cuvette for that experiment and had no detectable effect on the data analysis.

the values of the kinetic parameters obtained in this study are independent of the units used for $[P_1]$, the fluorescence intensities were used directly as pulses per second (pps). For reference, in this study the amount of MUGB hydrolyzed by 97 nM enzyme yielded an average fluorescence of 2.08 $\times$ 10^4 pps when the data were fit using eq 1 (extrapolated to infinite substrate concentration).

Time-dependent fluorescence data were collected at various MUGB concentrations (0.72−7.2 μM) at both pH 7.6 and pH 8.4, and initial estimates for the kinetic parameters were obtained as described under Experimental Procedures (*cf.* Figure 1). Using this method, it was possible to obtain convergence with well-defined parameters when fitting eq 1 globally to a complete set of assays. The best-fit curves resulting from these refinements are shown in Figure 2 for a series of assays obtained using various MUGB concentrations at pH 8.4. The refined final values of the kinetic parameters are summarized in Table 1, along with values obtained at pH 7.6. Kinetic parameter values reported for FVIIa in the absence of sTF were determined independently as described below.

Kinetic Parameters of MUGB Hydrolysis by FVIIa Alone. The formation of the acyl-enzyme intermediate using FVIIa in the absence of sTF occurred on a much longer time scale (~2100 s) than that observed with the sTF·FVIIa complex (~400 s) even at a comparatively high MUGB concentration (Figure 3). After approximately 35 min, addition of a saturating level of sTF caused only a slight, although rapid, increase in fluorescence (not shown). Under identical conditions, the sTF·FVIIa complex showed a burst several-fold greater in magnitude. This suggested that for FVIIa in the absence of sTF, the acyl-enzyme intermediate formed slowly over the course of the experiment and was essentially fully formed by 35 min. Thus, no burst was observed upon the addition of sTF. This conclusion was supported by the absence of amidolytic activity of MUGB-treated FVIIa, presumably due to the formation of a relatively stable acyl-FVIIa intermediate (see below). Two possibilities may account for the slow rate of acylation observed with FVIIa

Table 1: Summary of the Kinetic Constants Obtained for the sTF·FVIIa Complex Using Fluorescence Methods[a]

pH	K_s (M)	k_2 (s^{-1})	k_3 (s^{-1})	k_2/K_s $[(M\cdot s)^{-1}]$
7.6	$2.7\ (0.1) \times 10^{-5}$	$3.5\ (0.1) \times 10^{-2}$	$2.7\ (0.05) \times 10^{-4}$	1.3×10^3
8.4	$1.8\ (0.06) \times 10^{-5}$	$3.1\ (0.1) \times 10^{-2}$	$4.1\ (0.08) \times 10^{-4}$	1.7×10^3

[a] Values of k_2/K_s were calculated from the corresponding parameters. Numbers in parentheses denote standard errors obtained for each parameter from the fitting procedure.

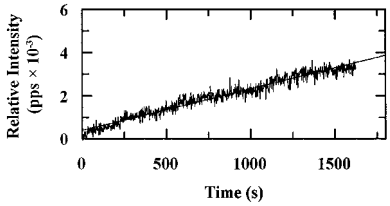

FIGURE 3: Typical time course for the hydrolysis of MUGB by FVIIa in the absence of sTF. The concentration of MUGB was 15 μM, and the concentration of FVIIa was 98 nM.

alone. One is that the rate constant for acylation may be much smaller for FVIIa alone than for the sTF·FVIIa complex, and the other is that K_s may be much higher in the absence of sTF.

Since obtaining values for K_s, k_2, and k_3 for MUGB hydrolysis by FVIIa alone was not possible by the same methods as described above for the sTF·FVIIa complex, alternative methods were required to determine these kinetic parameters. To estimate the affinity of MUGB for FVIIa in the absence of sTF, MUGB was treated as an inhibitor in initial velocity studies using the amide substrate Chromozym t-PA. This substrate is hydrolyzed approximately (1.5×10^3)-fold faster than the acylation rate for MUGB under the conditions used, as estimated from a comparison of k_2 at pH 8.4 for MUGB (Table 1) to k_{cat} for Chromozym t-PA under similar conditions (Neuenschwander et al., 1993) for the sTF·FVIIa complex.

MUGB inhibition data were fit using competitive, non-competitive, and uncompetitive modeling. In all cases, the

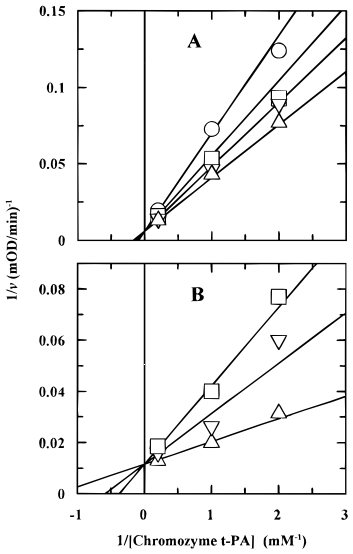

FIGURE 4: MUGB inhibition studies in double-reciprocal form. A series of chromogenic assays were performed at pH 8.4 as described under Experimental Procedures for FVIIa alone or the sTF·FVIIa complex with varied concentrations of MUGB as follows. FVIIa alone (panel A): 0 μM (△), 50 μM (▽), 100 μM (□), and 200 μM (○). The sTF·FVIIa complex (panel B): 0 μM (△), 10 μM (▽), and 20 μM (□). The lines are the best-fit lines from a global fit of eq 9 to each data set using nonlinear methods (GRAFIT; Leatherbarrow, 1992). The plots are presented in double-reciprocal form for clarity. The values of K_i determined from these data were 250 $\pm$ 20 μM for FVIIa alone and 8 $\pm$ 2 μM for the sTF·FVIIa complex.

competitive model was found to yield the best fits and was thus chosen for the remaining analyses. This model is described by the following standard initial velocity equation:

$$v = \frac{V_m[S]}{K_m(1 + [I]/K_i) + [S]} \quad (9)$$

where v is the velocity of the reaction expressed in unit concentration per unit time, V_m is the maximum velocity obtained at infinite substrate concentration, [S] is the experimental concentration of substrate, [I] is the experimental concentration of inhibitor, K_m is the Michaelis constant for substrate, and K_i is the inhibition constant for inhibitor.

MUGB acted as a competitive inhibitor of FVIIa alone, yielding a K_i of 250 $\pm$ 20 μM (Figure 4A). In the presence of sTF, MUGB also acted as a competitive inhibitor with an estimated K_i of 8 $\pm$ 2 μM at pH 8.4 (Figure 4B). Values of K_i for MUGB at pH 7.6 are given in Table 2. The K_i for MUGB with FVIIa alone was 31-fold higher than that for the sTF·FVIIa complex at pH 8.4, and 36-fold higher at pH 7.6.

The rate of deacylation of the acyl-FVIIa intermediate was determined directly as follows: For a substrate which yields a relatively stable (long-lived) acyl-enzyme intermediate, it is possible to reversibly inactivate the enzyme by a long incubation with the substrate. The acyl-enzyme can then be isolated by gel filtration, or it can be directly diluted into an assay mix containing a second substrate whose rate of hydrolysis is much faster than the first. The latter method is more convenient provided the residual first substrate does not effectively compete with the second substrate for enzyme active sites under the experimental conditions used. The time course of such an assay will show an initial exponential

Table 2: Summary of the Kinetic Constants Obtained for FVIIa Alone and the sTF·FVIIa Complex Using Alternative Methods[a]

enzyme	pH	K_i (M)	k_2 (s^{-1})	k_3 (s^{-1})	k_2/K_i [(M·s)$^{-1}$]
FVIIa	7.6	2.9 (0.5) $\times 10^{-4}$	2.7 $\times 10^{-2}$	4.9 (0.1) $\times 10^{-4}$	9.3 $\times 10^{1}$
	8.4	2.5 (0.2) $\times 10^{-4}$	ND	5.4 (0.1) $\times 10^{-4}$	
sTF·FVIIa	7.6	8 (1) $\times 10^{-6}$	3.4 (2.7) $\times 10^{-2}$	8.4 (0.07) $\times 10^{-4}$	4.3 $\times 10^{3}$
	8.4	8 (2) $\times 10^{-6}$	ND	6.9 (0.1) $\times 10^{-4}$	

[a] Values of K_i data were obtained experimentally from MUGB inhibition studies (see Figure 4). The values for k_3 were obtained directly by recovery of enzymatic activity of the acyl-enzyme intermediate. The value of k_2 for FVIIa alone was calculated as described in the text using K_i, k_3, the steady-state rate of MUGB hydrolysis from Figure 3, and eq 10. For comparison, the value of k_2 for the sTF·FVIIa complex was calculated as for FVIIa alone using the steady-state rates of MUGB hydrolysis from four independent determinations (Figure 2). The value shown is the mean and standard deviation obtained from the four determinations. Values of k_2/K_i were calculated from the corresponding parameters. ND denotes "not determined". With the exception of the values of k_2, numbers in parentheses denote standard errors obtained for each parameter from fitting procedures.

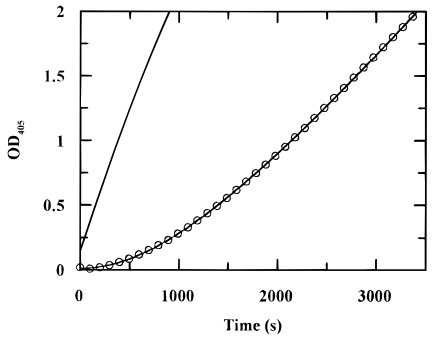

FIGURE 5: Time course for deacylation of the acyl-enzyme covalent complex (MUGB·sTF·FVIIa) measured at pH 7.6. The sTF·FVIIa complex was preincubated with MUGB for 60 min to form an acyl-enzyme intermediate, or not preincubated with MUGB. Hydrolysis of the chromogenic substrate, Chromozym t-PA, was then monitored by measuring the absorbance at 405 nm. In the absence of MUGB, the control assay shows a relatively linear rate of hydrolysis which represents full enzyme activity (line trace). The assay preincubated with MUGB shows the lag characteristic of slow recovery of active enzyme (○). The value of the rate constant for deacylation (k_3) determined for this experiment was 8.4 ($\pm$0.07) $\times 10^{-4}$ s^{-1}, which is in reasonable agreement with the value of k_3 derived from the fluorescence assay data (*cf.* Table 1).

increase in the rate of hydrolysis of the second substrate, which is a function of both the first-order generation of free enzyme via hydrolysis of the acyl-enzyme intermediate and the hydrolysis of the second substrate by the enzyme generated. The model used in this study (Scheme 2 under Experimental Procedures) is similar to that used for factor Xa (Bock et al., 1989), but with a derivation of the integrated rate equation similar in form to Wohl et al. (1978).

Results of a typical k_3 determination are shown in Figure 5 for the sTF·FVIIa complex at pH 7.6, with the best-fit curve using eq 6. Values of k_3 determined by this method at both pH values for the sTF·FVIIa complex and FVIIa alone are given in Table 2.

Experimental determination of the rate constant for acylation (k_2) of FVIIa alone was not possible due to the very slow rate of hydrolysis of MUGB, and absence of a pre-steady-state phase. However, by using the steady-state rate of hydrolysis of MUGB by FVIIa alone from Figure 3, it was possible to approximate k_2 for FVIIa at pH 7.6 based

on the above-determined values of K_i and k_3 using eq 10 which describes the steady-state rate of hydrolysis of substrate (v) as derived by Bender et al. (1967; eq 21) and solved for k_2.

$$k_2 = vk_3\left(\frac{[S]_0 + K_s}{[S]_0(k_3[E]_0 - v)}\right) \quad (10)$$

Values of k_2 calculated in this manner are shown in Table 2 for reference. The value of k_2 calculated for FVIIa alone was found to be very similar to that calculated for the sTF·FVIIa complex as well as the value of k_2 obtained experimentally for the complex (*cf.* Table 1), and cannot be considered significantly different. Thus, from the data presented in Tables 1 and 2, it can be seen that the predominant effect of sTF is to promote the formation of the MUGB−FVIIa complex by increasing the affinity of FVIIa for MUGB by 31−36-fold with little effect on the catalytic rate constants. The affinity of MUGB also shows a pH dependence, with the dissociation constant for the MUGB·enzyme complex being slightly higher at pH 7.6 than at pH 8.4.

DISCUSSION

Relationship between the Kinetic and Chemical Mechanisms of FVIIa. Although the kinetic mechanism for FVIIa has not been formally determined, all data accumulated on FVIIa kinetics are consistent with the general mechanism for trypsin-like serine proteases presented here as Scheme 1. In addition, this study presents good evidence for the formation of an acyl-FVIIa intermediate (see Figure 5 and description). The kinetic parameters determined for sTF·FVIIa at both pH 7.6 and pH 8.4 follow a pattern very similar to those obtained with other coagulation proteases using ester substrates, both chromogenic (Chase & Shaw, 1969; Smith, 1973) and fluorogenic (Livingston et al., 1981; Melhado et al., 1982). With sTF·FVIIa, the deacylation step for MUGB (represented by k_3) is rate-limiting since k_3 is about 2 orders of magnitude smaller than the acylation step (represented by k_2). Inherent in the model represented by Scheme 1 is the assumption that the release of P_1 is infinitely rapid and the ES′·P_1 complex does not exist. If the above assumption does not hold, the determined value of k_3 would actually be a bulk constant, reflecting the rate of release of P_1 and the deacylation step. In this study, we were able to verify the validity of the above assumption by independently determining k_3.

The k_2/k_3 ratio for sTF·FVIIa is 75 at pH 8.4 and 129 at pH 7.6. This is similar to the k_2/k_3 ratio of 34 determined for thrombin with a similar guanidinobenzoate fluorogenic substrate, but differs substantially from the ratios determined for trypsin (1.2×10^4) and plasmin (1.5×10^5) also using guanidinobenzoate fluorogenic substrates (Melhado et al., 1982). Kinetic rate constants for the chromogenic substrate *p*NPGB obtained with thrombin, trypsin, plasmin, and FXa (Chase & Shaw, 1969; Smith, 1973) show the same trend as the corresponding constants for fluorescent substrates. Based on the generally accepted mechanism for the serine proteases (Blow, 1976; Scheme 1), k_2 and k_3 represent the formation and decay of tetrahedral intermediates which are identical except that the intermediate associated with deacylation has water at the position formerly occupied by the leaving group. Thus, thrombin and FVIIa may share common structural elements distinct from the same elements in plasmin, trypsin, or FXa which contribute to the above phenomena. A detailed analysis of this awaits further structural information about FVIIa and the complexes formed with natural and synthetic substrates.

Effects of sTF on the Kinetic Mechanism of FVIIa. It is assumed that K_i and K_s both represent the same equilibria, and the observed effects of sTF on the K_i for MUGB are also reflected in the K_s for MUGB. Thus, the predominant effect of sTF on the hydrolysis of MUGB is to increase the affinity of the enzyme for MUGB by 31−36-fold (Tables 1 and 2). There are minor differences in the rate constants for the catalytic and product release steps. Similar observations have been made with FVIIa using *p*NPGB as a substrate (unpublished observations). This indicates that sTF assists in the productive binding of these substrates. Apparently, once the proper orientation of these substrates is achieved with respect to the catalytic triad, catalysis proceeds with minimal influence from sTF. These results are interesting when compared to the observed effects of sTF on the kinetics of hydrolysis of synthetic amide substrates where sTF elicits substantial k_{cat} effects (Neuenschwander et al., 1993; Butenas et al., 1993; Shigematsu et al., 1992). In contrast, there is only a minor change in k_{cat} [where $k_{cat} = k_2k_3/(k_2 + k_3)$] when MUGB is used as the substrate. However, sTF binding to FVIIa decreases the K_m for MUGB hydrolysis, paralleling the effects previously observed with some tripeptidyl substrates (Neuenschwander et al., 1993).

Energetics of sTF Binding. An allosteric effector may have very large effects on the catalytic rate constants of a particular reaction at the expense of very little binding energy, while an effector's ability to alter substrate binding affinity is limited by the number of binding interactions between effector and enzyme and the substrate and enzyme (Reinhart, 1983). For the interaction of a small ligand and a small substrate, the practical limit amounts to about a 30-fold effect on K_s. The results from this laboratory with both synthetic amide substrates (Neuenschwander et al., 1993) and an ester substrate (MUGB; Tables 1 and 2) show the maximum effect of sTF on K_s and k_{cat}/K_m of approximately 30−40-fold. For MUGB, a small substrate in a *K*-type system (Reinhart, 1983), this effect of sTF on k_{cat}/K_m is consistent with linkage theory since the limited number of binding contacts between MUGB and FVIIa will limit the magnitude of the sTF effect on K_s to about that observed experimentally.

A comparison of the apparent k_{cat}/K_m for FX activation by FVIIa in the absence and presence of sTF (without phospholipid) shows a (4×10^3)-fold to (5×10^3)-fold increase when sTF is present (Neuenschwander & Morrissey, 1994), compared to about a 30−40-fold increase for MUGB and tripeptidyl-amide substrates. However, activation of macromolecular substrates by TF·FVIIa likely involves substrate interactions remote from the active center of the enzyme. This possibility is supported by the recent identification of a putative substrate binding site on TF[2] (Roy et al., 1991; Ruf et al., 1992). Although catalysis effects should not be discounted, it is possible that the effect of sTF on proteolysis of FX by FVIIa may be more to assist in the

[2] Q. Huang, P. F. Neuenschwander, A. R. Rezaie, and J. H. Morrissey, manuscript submitted for publication.

binding interactions of the macromolecular substrate to FVIIa and affect the orientation of the substrate relative to the active site, as seen with MUGB, rather than to affect the catalytic steps directly.

ACKNOWLEDGMENT

We thank Eric S. Mills for excellent technical assistance.

REFERENCES

Bender, M. L., Kezdy, F. J., & Wedler, F. C. (1967) *J. Chem. Educ. 44*, 84−88.
Blow, D. M. (1976) *Acc. Chem. Res. 9*, 145−152.
Bock, P. E., Craig, P. A., Olson, S. T., & Singh, P. (1989) *Arch. Biochem. Biophys. 273*, 375−388.
Bom, V. J., & Bertina, R. M. (1990) *Biochem. J. 265*, 327−336.
Bom, V. J., Reinalda-Poot, J. H., Cupers, R., & Bertina, R. M. (1990) *Thromb. Haemostasis 63*, 224−230.
Butenas, S., Ribarik, N., & Mann, K. G. (1993) *Biochemistry 32*, 6531−6538.
Carson, S. D., & Brozna, J. P. (1993) *Blood Coagulation Fibrinolysis 4*, 281−292.
Chase, T., Jr., & Shaw, E. (1967) *Biochem. Biophys. Res. Commun. 29*, 512−514.
Chase, T. J., & Shaw, E. (1969) *Biochemistry 8*, 2212−2224.
Fiore, M. M., Neuenschwander, P. F., & Morrissey, J. H. (1994) *J. Biol. Chem. 269*, 143−149.
Harlos, K., Martin, D. M. A., O'Brien, D. P., Jones, E. Y., Stuart, D. I., Polikarpov, I., Miller, A., Tuddenham, E. G. D., & Boys, C. W. G. (1994) *Nature 370*, 662−666.
Higashi, S., Nishimura, H., Fujii, S., Takada, K., & Iwanaga, S. (1992) *J. Biol. Chem. 267*, 17990−17996.
Jameson, G. W., Roberts, D. V., Adams, R. W., Kyle, W. S. A., & Elmore, D. T. (1973) *Biochem. J. 131*, 107−117.
Kezdy, F. J., & Bender, M. L. (1962) *Biochemistry 1*, 1097−1106.
Krishnaswamy, S. (1992) *J. Biol. Chem. 267*, 23696−23706.
Lawson, J. H., Butenas, S., & Mann, K. G. (1992) *J. Biol. Chem. 267*, 4834−4843.
Leatherbarrow, R. J. (1992) GRAFIT Version 3.0, Erithacus Software Ltd., Staines, U.K.
Livingston, D. C., Brocklehurst, J. R., Cannon, J. F., Leytus, S. P., Wehrly, J. A., Peltz, S. W., Peltz, G. A., & Mangel, W. F. (1981) *Biochemistry 20*, 4298−4306.
Melhado, L. L., Peltz, S. W., Leytus, S. P., & Mangel, W. F. (1982) *J. Am. Chem. Soc. 104*, 7299−7306.
Muller, Y. A., Ultsch, M. H., Kelley, R. F., & de Vos, A. M. (1994) *Biochemistry 33*, 10864−10870.
Neuenschwander, P. F., & Morrissey, J. H. (1992) *J. Biol. Chem. 267*, 14477−14482.
Neuenschwander, P. F., & Morrissey, J. H. (1994) *J. Biol. Chem. 269*, 8007−8013.
Neuenschwander, P. F., Branam, D. E., & Morrissey, J. H. (1993) *Thromb. Haemostasis 70*, 970−977.
Rapaport, S. I. (1991) *Ann. N. Y. Acad. Sci. 614*, 51−62.
Reinhart, G. D. (1983) *Arch. Biochem. Biophys. 224*, 389−401.
Rezaie, A. R., Fiore, M. M., Neuenschwander, P. F., Esmon, C. T., & Morrissey, J. H. (1992) *Protein Expression Purif. 3*, 453−460.
Roy, S., Hass, P. E., Bourell, J. H., Henzel, W. J., & Vehar, G. A. (1991) *J. Biol. Chem. 266*, 22063−22066.
Ruf, W., Kalnik, M. W., Lund-Hansen, T., & Edgington, T. S. (1991a) *J. Biol. Chem. 266*, 15719−15725.
Ruf, W., Rehemtulla, A., Morrissey, J. H., & Edgington, T. S. (1991b) *J. Biol. Chem. 266*, 2158−2166 [correction in *J. Biol. Chem.* (1991) *266*, 16256].
Ruf, W., Miles, D. J., Rehemtulla, A., & Edgington, T. S. (1992) *J. Biol. Chem. 267*, 6357−6381.
Shigematsu, Y., Miyata, T., Higashi, S., Miki, T., Sadler, J. E., & Iwanaga, S. (1992) *J. Biol. Chem. 267*, 21329−21337.
Smith, R. L. (1973) *J. Biol. Chem. 248*, 2418−2423.
Waxman, E., Ross, J. B., Laue, T. M., Guha, A., Thiruvikraman, S. V., Lin, T. C., Konigsberg, W. H., & Nemerson, Y. (1992) *Biochemistry 31*, 3998−4003.
Wohl, R. C., Summaria, L., Arzadon, L., & Robbins, K. C. (1978) *J. Biol. Chem. 253*, 1402−1407.
Zur, M., & Nemerson, Y. (1978) *J. Biol. Chem. 253*, 2203−2209.

BI9529770